

Marine vibrator array design: an OBS example

Arash JafarGandomi, Sergio Grion and Sebastian Holland, Shearwater GeoServices

Summary

Marine seismic vibrators were introduced in the early 1970's but have not achieved wide commercial use probably due to the relative simplicity and versatility of marine air-gun sources. There has recently been a resurgence of interest in marine vibrators due to their low environmental impact and because they are more controllable and efficient than air-gun arrays. In this paper we discuss the optimal design of marine vibrator sweeps for ocean-bottom seismic surveys using a sweep generation approach guided by signal-to-noise ratio (SNR). As example, we use the SNR estimated from ocean bottom recordings in the North Sea. We describe a vibrator tow depth optimization approach based on the minimum achievable frequency and sweep length and design low- and high-frequency sweeps covering the 3-125Hz band.

Introduction

Marine seismic vibrators were introduced in the early 1970's (e.g., Broading et al., 1971). However, only recently have they been considered as a serious contender to air-gun arrays. While their reduced environmental impact is highly attractive (Southall et al., 2007; LGL and MAI, 2011; Southall et al., 2019), additional drivers are the ability to precisely control the characteristics of the released energy and the potential survey efficiencies that can be obtained (Halliday et al., 2018).

Currently, the most commonly used source type in marine seismic exploration is the air-gun array. Although it is theoretically possible to use an array of marine vibrators to match the down-going energy spectrum of an air-gun array,

putting the required hardware into the field is not practical. Instead, Laws (2012) proposed to use a requirement based on the target signal-to-noise ratio (SNR) of the final processed seismic image. A key requirement for the SNR estimation required by this approach is the acquisition of stealth test data, consisting of repeated navigation passes with active and inactive sources while receivers are constantly recording. Laws et al., (2018a) show that the spectrum of the marine vibrator sweep can be tailored to be the minimum needed to satisfy the imaging requirements. Laws et al., (2018a) used a SNR obtained from a towed streamer stealth test, while we here use the SNR estimated from a stealth test over ocean bottom cables (OBC) in the North Sea to design an array of marine vibrator sources and the corresponding sweeps.

Estimation of the target sweep spectrum

A key ingredient for generating sweeps is an estimate of SNR. To estimate the SNR, we carried out a stealth test by first shooting a seismic source line using conventional air-gun arrays with 25m source spacing over an OBC with 25m receiver spacing. Next, we repeated the line but this time without firing the sources. We then processed both datasets with the same processing flow. Comparing the spectrum of the two images at different depths provides us with estimates of SNR. It is important to keep the processing flow as deterministic as possible, to avoid the impact of data-driven processes on the estimated SNR.

The stealth test data consisting of a single line of receivers were processed using a basic fast-track flow. The main steps in the processing sequence were surface consistent

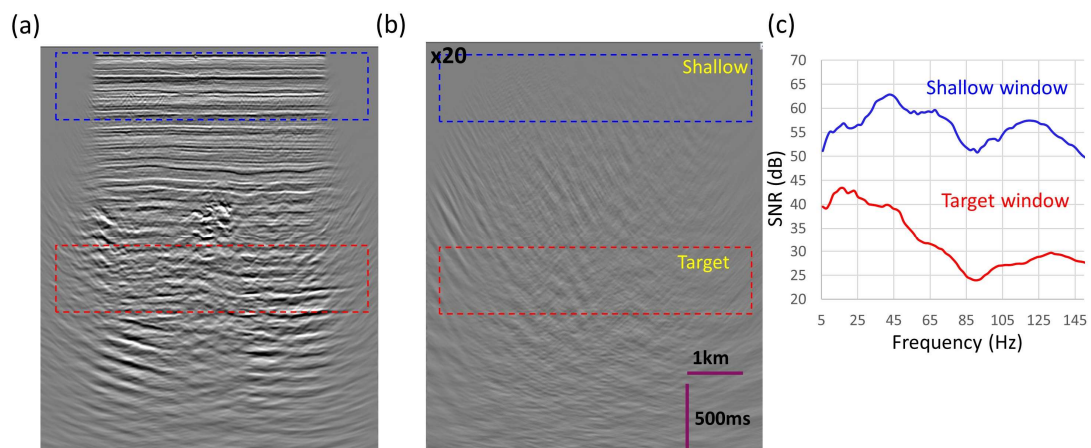


Figure 1. Migrated images from (a) active source recording and (b) the noise recording. (c) Estimated SNR spectra at shallow and target windows.

Marine vibrator array design

corrections, mute of seismic interference in the radon domain, de-signature and de-bubble, source de-ghosting, pre-direct arrival mute, offset regularization and pre-stack time migration.

Figure 1 shows the final migrated images (full-stack) and corresponding SNR spectra at shallow and target windows. The SNR in the shallow window is much higher than in the target window, and therefore we focus on the latter. This choice ensures that the image will be high quality from shallow to target depth. Once the SNR curves are estimated for each migrated offset, it is possible to evaluate their offset-dependency (not shown here). We observe that for this OBC acquisition the image quality decreases with increasing frequency (due to increased noise level at higher frequencies), depth and offset.

Since the stealth test is 2D, the estimated SNR must be adjusted for 3D survey design. Krey (1987) described an approach to estimate the SNR of 2D and 3D migrated images based on fold, migration aperture and size of the Fresnel zone. Following Krey's approach we calculate the ratio of 3D SNR to 2D SNR (SNR_{3D}/SNR_{2D}) with respect to frequency. For the desired 3D survey, we consider a source spacing of 25m in the inline direction (the same as the stealth test) and 50m in the crossline direction. The receiver spacing is 25m and 200m in the inline and crossline directions, respectively. For calculation of SNR_{3D}/SNR_{2D} we use the shorter dimension of the CDP (common-depth-point) bin size as 12.5m. These acquisition parameters lead to an increase of fold by a factor of 13 for a 3D survey over the 2D stealth test. We then calculate the expected SNR_{3D}/SNR_{2D} for a 45° migration aperture, which was the aperture used for the stealth test (Figure 2).

Since the SNR ratio shown in Figure 2 is calculated under simplistic assumptions (i.e., using straight rays and average root-mean-square velocity at the target), we take a conservative approach and use the lowest SNR scaling factor

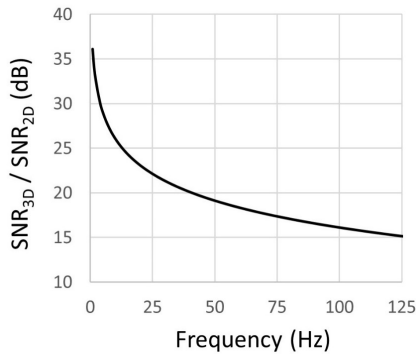


Figure 2. Variation of SNR_{3D}/SNR_{2D} with respect to frequency for 45° migration apertures.

of 15dB at the highest frequency of interest (125Hz). The corresponding value of 15dB is then added to the estimated SNR values at the target window to set the expected 3D SNR.

Next, we choose as target spectrum that of the 8m-depth air-gun array used for the stealth test, inclusive of source ghost at vertical incidence. Considering this typical 3-string, 3147 cubic inches air-gun array spectrum (dashed-line in Figure 3), it is possible to estimate a noise spectrum by subtracting the estimated SNR from the source spectrum, as shown in Figure 3 (dotted-line). To generate the required spectrum for the vibrator source-array, a certain desired SNR level for the final image needs to be defined, which can be frequency-dependent. The noise spectrum is then boosted by this value to create the desired vibrator array source spectrum. In this case we assume a desired 32dB SNR at the target level for all frequencies and the corresponding adapted spectrum is shown in Figure 3 (solid line).

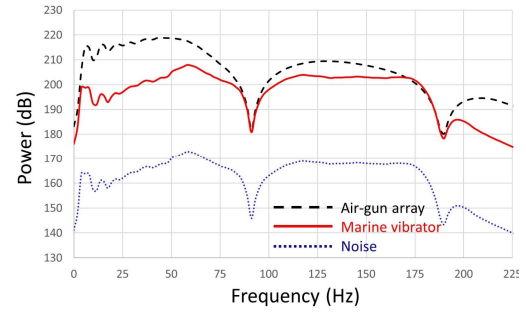


Figure 3. Generated target air-gun array spectrum (dashed-line), Marine vibrator spectrum (solid line) and noise spectrum (dotted-line). All spectra contain source-ghost for vertical incidence at 8m depth.

Sweep generation method

Having defined the required source energy spectrum, we then design a set of sweeps for an array of vibrators with various output characteristics. Following Rietsch (1977), we use the ratio between the required source power spectrum s_r and the monochromatic power response of the marine vibrator s_m to define the sweep rate $g(f)$,

$$g(f) = \frac{s_r}{\sum_{i=1}^N s_m^i}, \quad (1)$$

where N indicates the number of vibrator units. This rate is then integrated to give a monotonic frequency-sweep function $f(t)$.

To achieve the required minimum and maximum frequencies, we use an optimization approach. We pre-define the number of vibrators in each group, where each group emits a single sweep and is deployed at an optimal

Marine vibrator array design

depth. Additionally, we design continuous sweeps. The optimal depth is chosen to enhance the output energy from the vibrators array by accounting for the expected ghost response (Laws and Morice, 1999, Laws et al., 2018b). In general, high frequencies are emitted by vibrators deployed at shallower depths, and the low-frequency parts of the spectrum are emitted by vibrators deployed deeper. The optimal depth must be able to provide both minimum and maximum intended frequencies within the expected sweep time. With continuous sweeps, phase encoding can be used to remove residual shot noise (Laws et al., 2018b).

Optimization of vibrator array configuration

The range of required frequencies for each vibrator type affects the design of the array configuration. We use two sets of vibrators: low-frequency units limited to generate power in the range 3-25Hz and high-frequency units limited to generate 25-125Hz power. As the SNR-adapted spectrum (Figure 3) is less energetic at low-frequencies and more energetic at higher frequencies, it is expected that more vibrator units will be necessary for higher frequencies. This situation, which is specific to the SNR-based approach for this ocean-bottom case, is contrary to the traditional perception that marine vibrators are not suitable for the lower frequencies.

We use this design criteria and information on the performance characteristics of a marine vibrator system currently undergoing development to estimate the dependency of minimum sweep frequency and required sweep length on the deployment depths for low frequency and high frequency units. For a single low frequency unit, Figure 4a shows the variation of minimum achievable

frequency (while the maximum frequency is fixed at 25Hz and maximum sweep time is fixed at 25s) and the required sweep time to achieve the minimum frequency of 3Hz (Figure 4b) with respect to the depth of the low-frequency vibrator. This indicates that there is a high degree of freedom in choosing the depth of the low-frequency unit. However, this is not the case for the high-frequency units. Figure 4c and 4d present the same curves as in Figure 4a and 4b for the high-frequency vibrators using an array of 1, 2 and 3 vibrators while the maximum frequency is fixed to 125Hz. Figure 4c indicates that with two and three units the vibrators can be positioned shallower than 11m and 12m depth, respectively. However, to achieve a reasonable sweep time, the array of vibrators must be placed shallower than 6m (Figure 4c). For example, at 5m depth, the required sweep time to produce enough power within the frequency range of 25-125Hz is 13.7s, 6.9s and 4.6s for arrays of one, two and three vibrators, respectively. Inspection of Figures 4c and 4d indicates that either two or three high-frequency vibrators should be used in order to keep the sweep length below 10s.

We also examine the impact of splitting the high-frequency vibrators for the case of three vibrators to two different depth levels using two units for one set and a single unit for another set. Figure 5 shows the estimated sweep time for different combinations of depth levels for the two depth-groups. Compensating for the ghosts at different depth levels leads to a periodic pattern in both minimum achievable frequency and sweep length. Figure 5 indicates that putting the three units at the same depth of 5m leads to the shortest sweep length (4.6s) required to release the desired power and that at this depth there is some tolerance to depth variations. In Figure 5, the frequency range of the vibrators remains constant as the depth of deployment varies. One may of

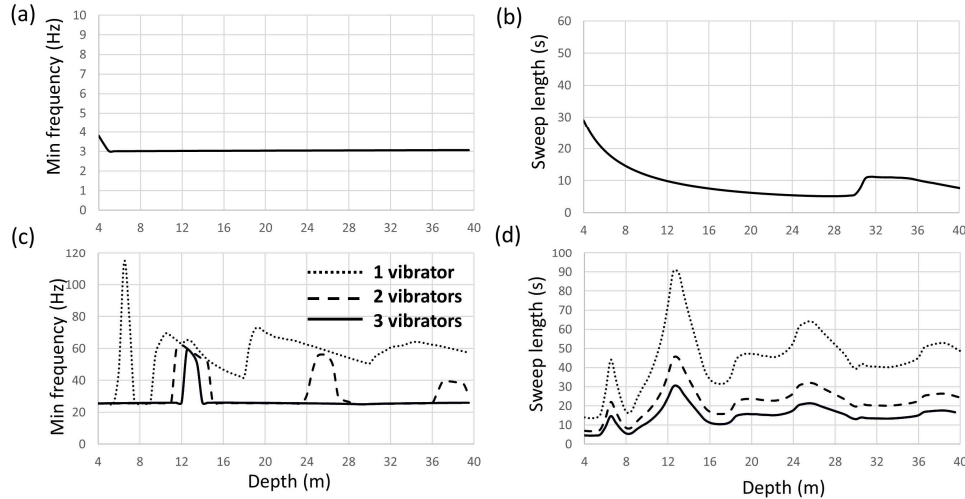


Figure 4. (a) and (b) variation of minimum achievable frequency within 25s sweep time and sweep length required to achieve minimum frequency with respect to depth for one low-frequency vibrator unit. (c) and (d) are same as (a) and (b), respectively, for high-frequency vibrator units in groups of 1, 2 and 3 units (in dotted, dashed and solid curves, respectively).

Marine vibrator array design

course modify the output frequency range for the high frequency units according to depth level, but this is not considered here.

Using the above optimization results, the optimum source configuration consists of two high-frequency vibrator units at 5m depth and a single low-frequency unit at a depth within the 20m-28m range. For the 20m case, the estimated sweeps and corresponding frequency-versus-time curves are shown in Figure 6.

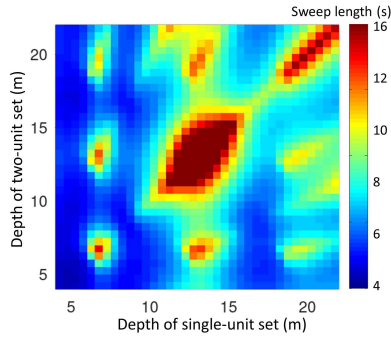


Figure 5. Estimated sweep length required to achieve minimum frequency (25Hz) for the high-frequency units with respect to the depth of the two vibrator groups.

Discussion

The optimal length of sweeps has a key impact on the survey design and particularly on the spacing between subsequent sweeps. For the survey parameters that we use here, we expect a 10s time-interval between subsequent sweep starts (assuming a boat speed of 4.9 knots), which is larger than the estimated optimal length for both sweeps. These 10s are consistent with the fold of the stealth test. However, vibrator units that can generate the 6.9s sweeps of Figure 6 can also

stretch their output along 10s if required, or alternatively operate every 6.9s for increased fold. The latter would result in a SNR improvement over the design target, and the sweep design process could be iterated to lower the output from the units. Iteration may also be required in case the optimal sweeps length become longer than the expected time-interval between the successive sweep points.

Conclusions

We discuss an approach to optimize an array of marine vibrators and generate corresponding SNR-based sweeps for an OBS survey. We indicate that due to the higher quality of the lower frequencies in OBS data compared to streamer data, a single marine vibrator can provide enough power to fulfill the sweep requirements within the frequency range of 3-25Hz. However, due to lower SNR at high frequencies, at least two marine vibrator units are required to achieve enough power within the frequency range 25-125Hz. We also show that putting the high-frequency units at the same depth leads to a shorter sweep length than putting them in two separate depth-groups, when their output frequency range is fixed.

Acknowledgements

We thank Equinor and the Research Council of Norway for the financial support that makes this work possible. We also thank Lundin Energy Norway for providing us with the showrights for the stealth test data. The authors would like to acknowledge Robert Laws and Shearwater personnel involved in arranging and acquiring the stealth test data and thank Shearwater for permission to publish this work.

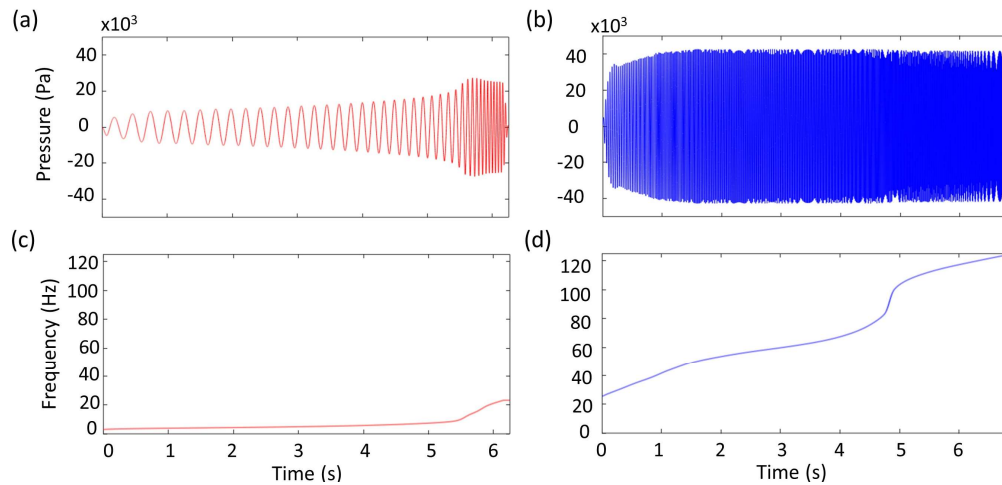


Figure 6. Generated sweeps for the (a) low-frequency and (b) high-frequency vibrator units. (c) and (d) corresponding frequency versus time functions for the low- and high-frequency vibrators, respectively.